

A simulation study of ventilation and indoor gaseous pollutant transport under different window/door opening behaviors

Weihui Liang (✉), Menghao Qin

School of Architecture and Urban Planning, Nanjing University, Nanjing 210093, China

Abstract

The window/door opening behavior of occupants is a very important factor in determining the airflows and ventilation conditions in buildings, on which indoor pollutant concentration and transport are highly dependent. A two-room residence model was simulated in this study to analyze the airflow characteristics and pollutant transport under different window/door opening behaviors. Airflows were unidirectional and the residence could not be treated as a well-mixed zone when there were no temperature differences. If there were temperature differences, two-way airflow occurred at the exterior window of the room when it was open and the interior door was closed, resulting in a much larger ventilation rate than the situation without temperature differences. Strong two-way airflow occurred at the interior door in the case of the exterior window closed and interior door open, as the air in the two connected rooms was well mixed after the interior door was opened for tens of minutes. The ventilation rate of the room with double-sided ventilation was much higher than that of the room with single-sided ventilation, even though the total opening areas were the same. Opening the exterior window and closing the interior door could effectively remove pollutants from a polluted room and prevent their transport to a clean room. Field experiments were performed and the main conclusions of the simulation were verified.

1 Introduction

Occupants spend a substantial fraction of their time indoors (Brasche and Bischof 2005) and thus, indoor air quality (IAQ) plays a significant role in human health. The control of window/door openings is one of the most convenient approaches for occupants to remove indoor pollutants and prevent their transport to other indoor areas. Exterior and interzonal airflows were influenced by window/door opening behaviors, affecting indoor pollutant variation, transport from indoor to outdoor, and movement between rooms (Johnson et al. 2004; Canha et al. 2016). Understanding airflow characteristics under different window/door opening behaviors is very important for maintaining good IAQ.

Natural ventilation is a very common ventilation strategy in buildings when outdoor environmental conditions are favorable (Taheri et al. 2016). The driving force of natural ventilation could be created by exterior wind and an indoor-to-outdoor temperature difference (Teclé et al. 2013; Nabi

and Flynn 2015; Tlili et al. 2015). Inter-room temperature difference could also induce two-way airflow at the interior door, causing pollutants to be transported between rooms (Chen et al. 2011). Natural ventilation rate depends on the meteorological conditions (Isaacs et al. 2013), building characteristics (Dodson et al. 2007; Nantka 2005), and occupants' window/door opening behaviors (Howard-Reed et al. 2002). For a determined building, the window/door opening behavior is a factor that could be more easily controlled by the occupant themselves. This behavior could strongly influence the flow resistance of the building and this, in turn, would have a strong influence on airflow, pollutant variation, and occupant indoor exposure (Wilson et al. 1996; Liang and Yang 2013; Chen et al. 2012a). Studies on the airflow and pollutant variation under different window/door opening behaviors are very important for providing recommendations of the appropriate window/door opening behaviors from a pollutant control and removal perspective.

Exterior airflows across the exterior envelopes of buildings

Keywords

two-way airflow, pollutant transport, well-mixed, single-sided ventilation, temperature difference

Article History

Received: 22 August 2016
Revised: 24 October 2016
Accepted: 26 October 2016

© Tsinghua University Press and Springer-Verlag Berlin Heidelberg 2016

have been extensively studied. An open exterior window could increase the ventilation rate several fold, depending on the width of the opening and the number of opened windows (Howard-Reed et al. 2002). Pollutant concentration from indoor sources decreases when exterior windows are opened, whereas it increases when windows and doors are closed (Liang and Yang 2013). Interior airflows across interior doors could be unidirectional or bidirectional. Miller and Nazaroff (2001) measured the airflow in a two-zone test space and reported that the two-way airflow rate was over $100 \text{ m}^3/\text{h}$ when the interior door was wide open, whereas the rate decreased to $\sim 1 \text{ m}^3/\text{h}$ when it was closed. Ferro et al. (2009) found that closing an interior door could effectively prevent the transport of air pollutants. Chen et al. (2011) claimed that the two-way airflow played an important role in pollutant transmission when temperature differences occurred. McGrath et al. (2014) simulated $\text{PM}_{2.5}$ concentrations due to interzonal airflow and found that both the time of occurrence and duration of the interzonal airflow were critical to the indoor concentration. However, most studies have analyzed the influences of exterior windows and interior doors separately, thus studies on the airflow and pollutant variation under different window/door opening behaviors are lacking.

The main objectives of this study were to: (1) characterize the exterior and interzonal airflows under different window/door opening behaviors, (2) analyze the gaseous pollutant transport and air mixing conditions between rooms, and (3) develop some guidelines for occupants regarding window/door opening behavior from a pollutant control perspective. The multi-zone software CONTAM 2.4 was used to simulate the airflows. Indoor pollutant concentrations under some typical cases were also analyzed. Field experiments were performed in a three-room residence and the data from such were compared with the simulation results.

2 Materials and methods

2.1 Simulation scenarios

Figure 1 shows a schematic illustration of the studied residence model. It is a two-room residence, which represents the simplest multi-room scenario in reality. Exterior airflows from outdoor to indoor, interzonal airflows between rooms, and the mixing condition of pollutants under different window/door opening behaviors could all be studied. Other multi-room residences could be treated as several two-room residence units connected by interior doors. Consequently, the two-zone model is widely used to analyze interzonal airflows and pollutant transport in the literature (Du et al. 2015; Ott et al. 2003).

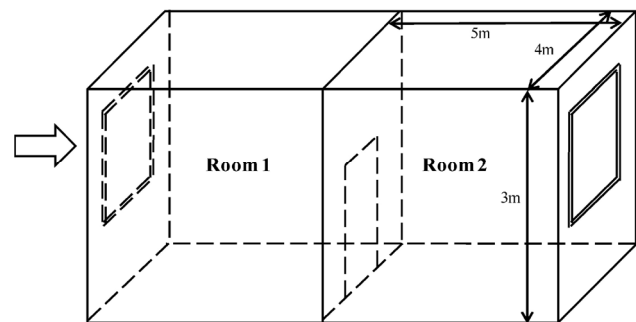


Fig. 1 Schematic illustration of the two-room residence model

As shown in Fig. 1, the dimensions of each room of the residence are the same, $5 \text{ m} \times 4 \text{ m} \times 3 \text{ m}$ (length \times width \times height). A sliding window of dimensions $2 \text{ m} \times 2 \text{ m}$ is presented in the exterior wall of each room, one of which is facing the direction of the outdoor wind, whereas the other is on the opposite side. Only half of the total area could be open. An interior door with dimensions $2 \text{ m} \times 1 \text{ m}$ (height \times width) connects Rooms 1# and 2#. To simplify the situation, outdoor temperature, velocity, and indoor temperature of the rooms were set as constant during each simulation case. Room 1# was used as the reference room and was set to a constant outdoor temperature of $26 \text{ }^\circ\text{C}$. This outdoor temperature condition is very favorable for natural ventilation, which leads to a high possibility for an occupant to open a window/door. The temperature of Room 2# was higher than Room 1#, which could be determined by the temperature difference between rooms (Δt). Other parameters, such as the outdoor wind velocity (v), effective air leakage area coefficient (C_{ed} for door and C_{ew} for window) of the closed openings, opening area ratio of the exterior window (R_{area}), and opening angle of the interior door (A_{angle}), were varied so their influences on airflows could be studied. The selected values of these parameters are summarized in Table 1. The total number of airflow simulation cases was 972. Four different window/door opening behaviors, i.e., exterior window open and interior door closed, exterior window closed and interior door open, exterior window open and interior door open, and exterior window closed and interior

Table 1 Summary of parameters in the two-room residence model

Parameters	Selected values	Remarks
v (m/s)	0, 2, 4, 6, 8, 10	Outdoor air velocity
C_{ew} (cm^2/m^2)	0.3, 5.3, 10.3	Effective air leakage area coefficient of exterior window
C_{ed} (cm^2/m^2)	2.4, 12, 25	Effective air leakage area coefficient of interior door
R_{area}	0.1, 0.5	Opening area ratio of exterior window
A_{angle}	5° , 45° , 90°	Opening angle of interior door
Δt ($^\circ\text{C}$)	0, 1, 2	Temperature difference between rooms

door closed, were analyzed. They represent the most common window/door opening behaviors in reality.

2.2 Theoretical models for calculating airflows

The multi-zone software CONTAM was used to analyze the airflow and ventilation rate under different window/door opening behaviors. This software has been widely used for airflow and ventilation simulations in buildings (Persily et al. 2010; Shi et al. 2015; Viegas et al. 2015; Dols et al. 2016). The accuracy of the simulation has also been validated (Emmerich et al. 2004). The airflow models and flow resistances in this study were determined as follows.

2.2.1 Airflow model for large openings

The widely used power law and quadratic models allow flow in only one direction at a time. When a window or door is open, it is a large opening and airflow through it tends to be complex. The temperature difference between rooms will result in an air density difference, leading to a positive pressure difference at the top of the opening and a negative pressure difference at the bottom (or vice versa) (Dols et al. 2013). Under this condition, two-way airflow may occur. Equations (1) and (2) are used to describe the two-way airflow model for the large opening (Dols et al. 2013).

$$Q_{i-j} = \frac{2}{3} C_d W \sqrt{\frac{2g|\Delta\rho|}{\rho}} \left(\frac{H}{2} + Y\right)^{\frac{3}{2}} \quad (1)$$

$$Q_{j-i} = \frac{2}{3} C_d W \sqrt{\frac{2g|\Delta\rho|}{\rho}} \left(\frac{H}{2} - Y\right)^{\frac{3}{2}} \quad (2)$$

where Q_{i-j} and Q_{j-i} are the airflow rates from zone i to zone j , and zone j to zone i , respectively; W is the width of the opening; g is the acceleration of gravity; $\Delta\rho$ is the air density difference between zones; H is the overall height of the opening; Y is the neutral height, where the air velocity is zero; and C_d is the discharge coefficient of the opening. In this study, C_d for the opened sliding window was set to 0.78, based on the experiments by Weber and Kearney (1980), whereas for the opened interior door, C_d is dependent on the opening angle (θ). According to the experimental data by Yang et al. (2010), C_d could be calculated by the following equation (Yang et al. 2010):

$$C_d = 0.0256 \times \theta^{0.7432} \quad (3)$$

In Eqs. (1) and (2), when $|Y| < H/2$, there is two-way airflow and the ventilation rate through the opening could be calculated. When there is no possibility of two-way airflow, different formulae are used in the CONTAM simulation (Dols et al. 2013).

2.2.2 Airflow model for closed openings

When the window or door is closed, the opening could be equivalent to two horizontal and two vertical cracks. The height of the horizontal cracks and width of the vertical cracks are the same, which could be calculated as (Chen et al. 2012b):

$$h = \frac{HWC_e}{20000(H+W)} \quad (4)$$

where C_e is the effective air leakage area coefficient of the opening. In this study, the effective air leakage area coefficient of the window (C_{ew}) and door (C_{ed}) varied among the three different values listed in Table 1, which represent the smallest, mean, and largest values, according to the ASHRAE Handbook (ASHRAE 2001).

For horizontal air leakage, the height of the crack is too small to induce two-way airflow, thus a one-way power law model is used. The relationship between airflow rate ($Q_{h,i}$) and pressure difference ($\Delta P_{h,i}$) could be expressed as (ASHRAE 2001):

$$Q_{h,i} = \frac{C_{D,ref} A_{eff,h}}{10000} \sqrt{\frac{2}{\rho}} (\Delta P_{ref})^{-0.15} (\Delta P_{h,i})^{0.65} \quad (5)$$

where $C_{D,ref}$ is the reference discharge coefficient, which has a value of 1; and ΔP_{ref} is the reference pressure difference, which is 4 Pa. $A_{eff,h}$ is the effective area, which can be expressed as:

$$A_{eff,h} = Wh \quad (6)$$

where W is the width of the opening, which is 1 m for the interior door and 2 m for the exterior windows; and h is the height of the horizontal air leakage calculated by Eq. (4). For vertical air leakage, the two-way airflow model of Eqs. (1) and (2) was used, in which C_d was set to 0.78 and the width of the vertical crack calculated using Eq. (4). These airflow models have been experimentally validated (Chen et al. 2011, 2012b).

2.3 Pollutant simulation

In addition to the airflow and ventilation rate, emission source is another key factor influencing the concentration and mixing condition of indoor pollutants. Short-term sources from tobacco smoke or cooking and long-term sources from building materials present different characteristics. Indoor pollutant variation and the mixing condition between rooms would be different due to the source differences, even under the same window/door opening behavior. Detailed analysis of the indoor pollutant variation and mixing level with different kinds of emission sources is beyond the scope of

this study. Only a short-term emission source, which resulted in a high initial pollutant concentration in the polluted room, was simulated. The clean room with low initial concentration was the receptor room. Previous studies have indicated that the short emission period of source and the rapid intra-room mixing could assure a reasonably well-mixed condition within a room (Ferro et al. 2009; Baughman et al. 1994), which perfectly meets the assumption of the multi-zone model. We focused on room-to-room pollutant variability and mixing rather than on within-room mixing, thus a multi-zone model was used. Normalized pollutant concentrations of 5 units for the polluted room and 1 unit for outdoor and the receptor room were used. The pollutant was removed only by airflows and not by deposition or reaction; a sink effect was not considered. Two scenarios with high initial concentration in Room 1# or Room 2# were analyzed. By inputting the multi-zone airflow and ventilation simulation results of CONTAM, indoor pollutant concentrations were simulated based on the mass balance equations.

2.4 Experimental setup

To validate the room-to-room pollutant variation patterns under different window/door opening behaviors, field experiments were performed in a three-room residence in Beijing. CO₂ was used as the tracer gas to represent the gaseous pollutant. The layout of the residence, with dimensions 9 m × 5 m × 3 m (length × width × height), is illustrated in Fig. 2. Room 1# and Room 2#, Room 2# and Room 3# could be treated as a two-room residence similar to the simulation model described in Section 2.1. The windows of the residence are sliding windows and only half of the total area could be opened.

At the beginning of the experiment, all the windows and doors were kept closed, and a pressurized cylinder containing CO₂ was used as the short-term emission source. The emission

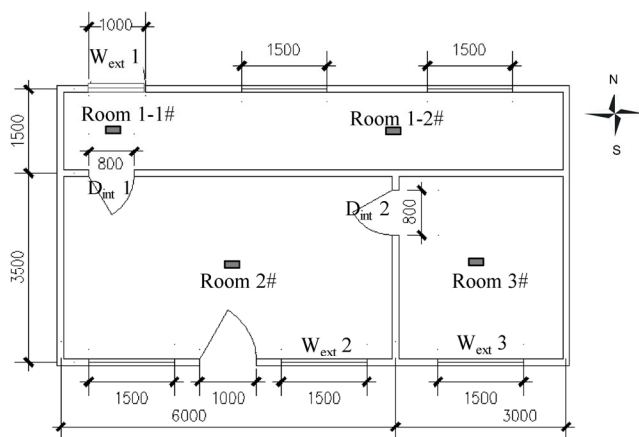


Fig. 2 Layout of the three-room experimental residence (■: positions of the CO₂ and temperature measurement instruments)

rate was not controlled, but the total emission time was within 10 min, resulting in ~2000 ppm initial CO₂ concentration in the source room. After the indoor CO₂ concentration changed very slowly and became relatively steady, the window/door of the residence switched from the closed positions to the desired positions. Then, the tester went outdoors immediately, thus the CO₂ emissions from them could be neglected after adjusting the window/door. A Telaire 7001 measured the CO₂ concentrations at an interval of 20 s. The instruments were placed in the centers of Room 2# and Room 3#, 1.5 m above the floor. The other two were placed in different locations of Room 1# to verify the mixing condition within the room. The measurement range and error of the instrument are 0–2500 ppm and 50 ppm, respectively. Outdoor CO₂ concentration was around 490 ppm, as recorded by the instrument. Indoor and outdoor temperatures varied naturally and were measured continuously at an interval of 10 min by an automatic data logger (WWZY-1 sensor, Beijing, China). The instrument measurement range and error were –20 to 80 °C and 0.3 °C, respectively. Detailed positions of the instruments are presented in Fig. 2. The outdoor wind direction and speed were measured by a local weather station (BJ7R-DYYZII-RTF), 2 m above the roof of the residence. The measurement ranges of wind direction and wind speed were 0–360° and 0–60 m/s, respectively.

Two different scenarios were measured on two different days in the winter season, with each of them lasting about 1 h. In the first experimental scenario, Room 2# was the polluted room and Rooms 1# and 3# were the receptor rooms. The interior door ($D_{int 1}$) connecting Rooms 1# and 2# was opened, whereas the others were closed. Pollutant variations in Room 2# and Room 1# could be used to investigate pollutant transport using the exterior window closed and interior door open behavior, whereas that in Room 2# and Room 3# could be used to examine pollutant transport using the exterior window closed and interior door closed behavior. In the second experimental scenario, Rooms 2# and 3# were the polluted rooms and Room 1# was the receptor room. $W_{ext 1}$, $D_{int 1}$, $W_{ext 2}$, and $W_{ext 3}$ were opened and the others were closed. Pollutant variations in Room 2# and Room 1# could be used to investigate pollutant transport using the exterior window open and interior door open behavior. Pollutant variations in Room 2# and Room 3# could be used to examine pollutant transport using the exterior window open and interior door closed behavior. The opening area ratio for an exterior window (R_{area}) was 0.1 and the opening angle for an interior door was 90°. Airflows of the experimental scenarios were analyzed by CONTAM using the measured boundary conditions, and indoor CO₂ concentrations were also simulated and compared with the measurement data.

3 Results and discussion

3.1 Simulation results of the two-room residence

3.1.1 Exterior window open and interior door closed

When $\Delta t = 0^\circ\text{C}$, there was no temperature difference between rooms, and indoor temperatures were also identical to those outdoors. Airflows at all the openings were unidirectional. The airflow direction was from the windward to the leeward, meaning from outdoor to Room 1# and then from Room 1# to Room 2#. The air change rates per hour (ACHs) for outdoor to Room 1#, Room 1# to Room 2# and Room 2# to outdoor were identical and are shown in Fig. 3(a). ACHs of the rooms were linear to outdoor wind velocity and the values were lower than 1 h^{-1} . Increasing the opening area ratio of the exterior windows could barely increase ACH, whereas it increases as the effective air leakage coefficient of interior door (C_{ed}) increases. This is because the flow resistance of a closed door is much larger than that of open windows, thus the overall flow resistance of the residence was mainly dependent on the door.

When an indoor temperature difference occurred between Room 1# and Room 2#, the temperature in Room 1# and the temperature difference between Room 1# and outdoor remained unchanged. The airflow pattern at the exterior window and interior door of Room 1# remained the same as the conditions lacking a temperature difference. The ACHs from outdoor to Room 1# and Room 1# to Room 2# were almost the same as Fig. 3(a) shows. The airflow and ventilation rate in the room with a temperature difference (Room 2#) were significantly different from the room without a temperature difference (Room 1#). Two-way airflow occurred at the exterior window of Room 2#, resulting in a larger ventilation rate than in Room 1#. The ACH from outdoor to Room 2# is given in Fig. 3(b). It decreased slightly as the outdoor wind velocity increased. A temperature difference greatly affects ACH, which increased about 40% when Δt increased from 1°C to 2°C . Different from Room 1#, the ACH of Room 2# was more sensitive to the changes of an opening area ratio of the exterior window than to the changes in the air tightness of the interior door.

Based on the airflow results at $\Delta t = 0^\circ\text{C}$, the airflow directions were the same and the main differences among these cases were in the value of ACH. Thus, pollutant concentration may differ case-by-case, but the variation and transport might share the same patterns. The pollutant concentration at $R_{area} = 0.1$, $C_{ed} = 25\text{ cm}^2/\text{m}^2$, and $v = 4\text{ m/s}$ with an ACH about 0.28 h^{-1} was simulated and used as a representative case and is shown in Fig. 3(c). The pollutant was transported in the same direction as the airflows due to the unidirectional characteristics. The pollutant in Room 1# was transported to Room 2# and increased in concentration

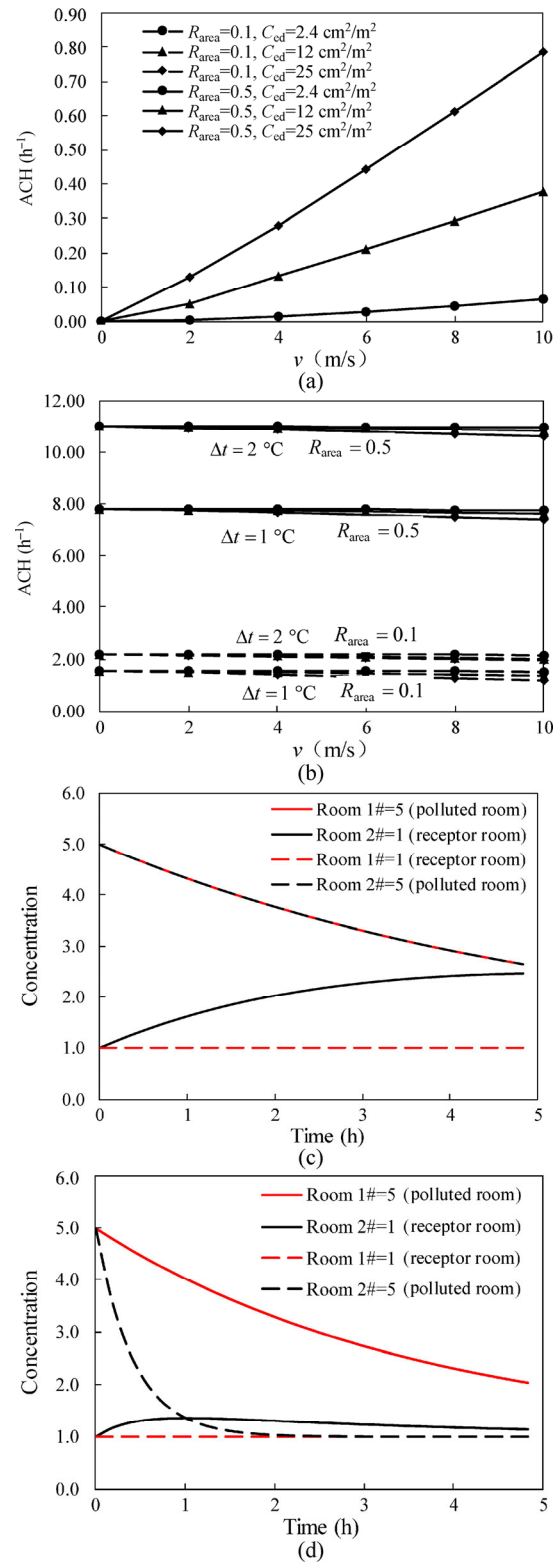


Fig. 3 ACH and indoor pollutant simulation results of the two-room model using the exterior window open and interior door closed behavior. (a) ACHs from outdoor to Room 1#, Room 1# to Room 2#, and Room 2# to outdoor with $\Delta t = 0^\circ\text{C}$; (b) ACH from outdoor to Room 2#; (c) indoor pollutant variations of the rooms with $\Delta t = 0^\circ\text{C}$; (d) indoor pollutant variations of the rooms with $\Delta t = 2^\circ\text{C}$

when the polluted room (Room 1#) was in the upstream position, whereas the pollutant in Room 2# could not be transported to Room 1# when the polluted room (Room 2#) was in the downstream position. The pollutant concentration in Room 1# remained unchanged, whereas pollutant variation in Room 2# was the same as that in Room 1# in the upstream polluted room scenario. The reason for this could be that when there is no source in Room 1# and the initial pollutant concentration is the same as outdoors, the fresh air would not be polluted after flowing through Room 1#. Due to these variation characteristics, when $\Delta t = 0\text{ }^\circ\text{C}$, indoor pollutant concentrations for the downstream polluted room scenario were not further simulated and discussed for other window/opening behaviors. Concentration differences between rooms are significant no matter which polluted room is in the upstream or downstream position. The two-room residence could not be treated as a well-mixed zone.

When a temperature difference occurred between rooms, the airflow and ACH of the rooms changed and thus the pollutant might vary differently. The pollutant concentration at $R_{\text{area}} = 0.1$, $C_{\text{ed}} = 25\text{ cm}^2/\text{m}^2$, and $v=4\text{ m/s}$ with $\Delta t = 2\text{ }^\circ\text{C}$ was simulated and is shown in Fig. 3(d). The ACHs from outdoor to Room 1# and outdoor to Room 2# were 0.28 h^{-1} and 2.11 h^{-1} , respectively. The pollutant concentration in Room 1# was the same as in Fig. 3(c) because airflow directions and the ACH of Room 1# did not change. The two-way airflow induces more fresh air to be exchanged at the exterior window of Room 2# and the concentration in Room 2# decreased rapidly and was lower than the situation lacking a temperature difference (black dash line in Fig. 3(c) vs. Fig. 3(d)). The closed interior door effectively prohibited pollutant transport between rooms (dash line in Fig. 3(d)). The concentration difference between rooms was obvious and the residence could not be treated as well mixed.

As temperature difference between indoor and outdoor is a common phenomenon in reality, two-way airflow at an opened exterior window could happen. When emission sources are in the room, it is highly recommended to open the exterior window of the polluted room to increase the ventilation rate and eliminate the indoor pollutants, whereas an interior door connecting the polluted room to others should be closed to prevent transport of the pollutant to those rooms.

3.1.2 Exterior window closed and interior door open

At the condition with $\Delta t = 0\text{ }^\circ\text{C}$, the ACHs from outdoor to Room 1#, Room 1# to Room 2#, and Room 2# to outdoor were identical and are shown in Fig. 4(a). The air tightness of an exterior window (C_{ew}) greatly affects ACH, whereas the effect of the opening angle of the interior door could be neglected. The ACHs of the rooms are smaller than 1 h^{-1} , close to the exterior window open and interior door closed scenarios.

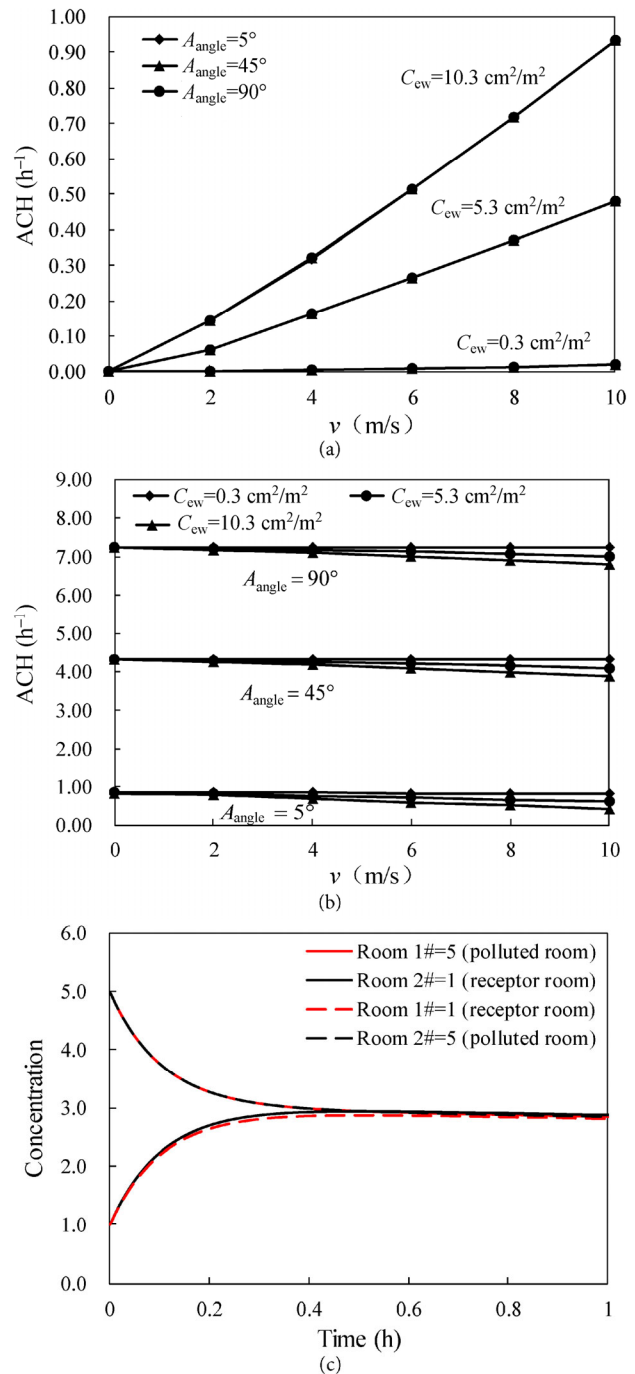


Fig. 4 ACH and indoor pollutant simulation results of the two-room model using the exterior window closed and interior door open behavior. (a) ACHs from outdoor to Room 1#, Room 1# to Room 2#, and Room 2# to outdoor with $\Delta t = 0\text{ }^\circ\text{C}$; (b) ACH from Room 2# to Room 1# with $\Delta t = 1\text{ }^\circ\text{C}$; (c) indoor pollutant variations of the rooms with $\Delta t = 1\text{ }^\circ\text{C}$ and $A_{\text{angle}} = 45^\circ$

When the temperature differed between rooms, the airflows at the exterior windows of Rooms 1# and Room 2# were unidirectional. Ventilation rates from outdoor to Room 1# and Room 2# to outdoor were almost the same as those when no temperature difference was present. However,

two-way airflow occurred at the interior door. The ACH from Room 2# to Room 1# with $\Delta t = 1\text{ }^\circ\text{C}$ is illustrated in Fig. 4(b). It shares the same variation pattern and increased about 40% when Δt increased from $1\text{ }^\circ\text{C}$ to $2\text{ }^\circ\text{C}$. The two-way airflow rate at the interior door was much larger than the values at the exterior windows. The opening angle of the interior door is an important factor to the two-way airflow rate. The leakage area of the exterior window (C_{ew}) and the outdoor wind velocity have negative effects on the two-way airflow rate, but these effects are not significant.

When $\Delta t = 0\text{ }^\circ\text{C}$, the airflow directions were the same and the ACHs of the rooms were close to the exterior window open and interior door closed scenarios. Indoor pollutant concentrations were supposed to share the same features as discussed in Section 3.1.1 and are shown in Fig. 3(c). Thus, indoor pollutant concentrations with $\Delta t = 0\text{ }^\circ\text{C}$ were not repeated here. When there was a temperature difference, two-way airflow occurred at the opened interior door. Pollutant concentrations at $C_{ew} = 5.3\text{ cm}^2/\text{m}^2$, $A_{\text{angle}} = 45^\circ$, and $v = 4\text{ m/s}$ with $\Delta t = 1\text{ }^\circ\text{C}$ were simulated and are shown in Fig. 4(c). No matter if the polluted room is in the upstream or downstream position, the indoor pollutant is transported from the polluted room to the receptor room, driven by the two-way airflow. Thus, concentrations in the polluted room decreased, whereas those in the receptor room increased. The concentration difference between Room 1# and Room 2# decreased with time, as the concentrations were close to each other after the interior door had been opened for over 20 min. Consequently, the two-room residence could be treated as a well-mixed zone. Under conditions with larger temperature differences or opening angles, the two-way airflow rate would be larger and the air would be well mixed in a shorter time. From a pollutant control perspective, this window/door opening behavior is not recommended because the pollutant in the polluted room could not be eliminated effectively and was transported to the receptor room in a short time.

3.1.3 Exterior window open and interior door open

When the exterior windows and interior door were open and no temperature difference was present, airflows through all the openings were unidirectional and the directions were the same as discussed in Section 3.1.1. The ACHs from outdoor to Room 1#, Room 1# to Room 2#, and Room 2# to outdoor were identical and are shown in Fig. 5(a). The ACH for this situation was the largest among all the window/door opening behaviors, and was larger than 10 h^{-1} in most cases. Increasing the opening area ratio of an exterior window and the opening angle of an interior door could increase the ACH. By comparing the ACHs of Fig. 3(a) and Fig. 4(a) with Fig. 5(a), one sees that the ACH of the room with double-sided ventilation was much larger than it was for a room

with single-sided ventilation. Moreover, as the ACH of the room barely increased with the increase of opening area ratio of the window and opening angle of the door at single-sided ventilation situation, it should be more effective for increasing ACH to increase the number of the opened openings than to increase the opening area.

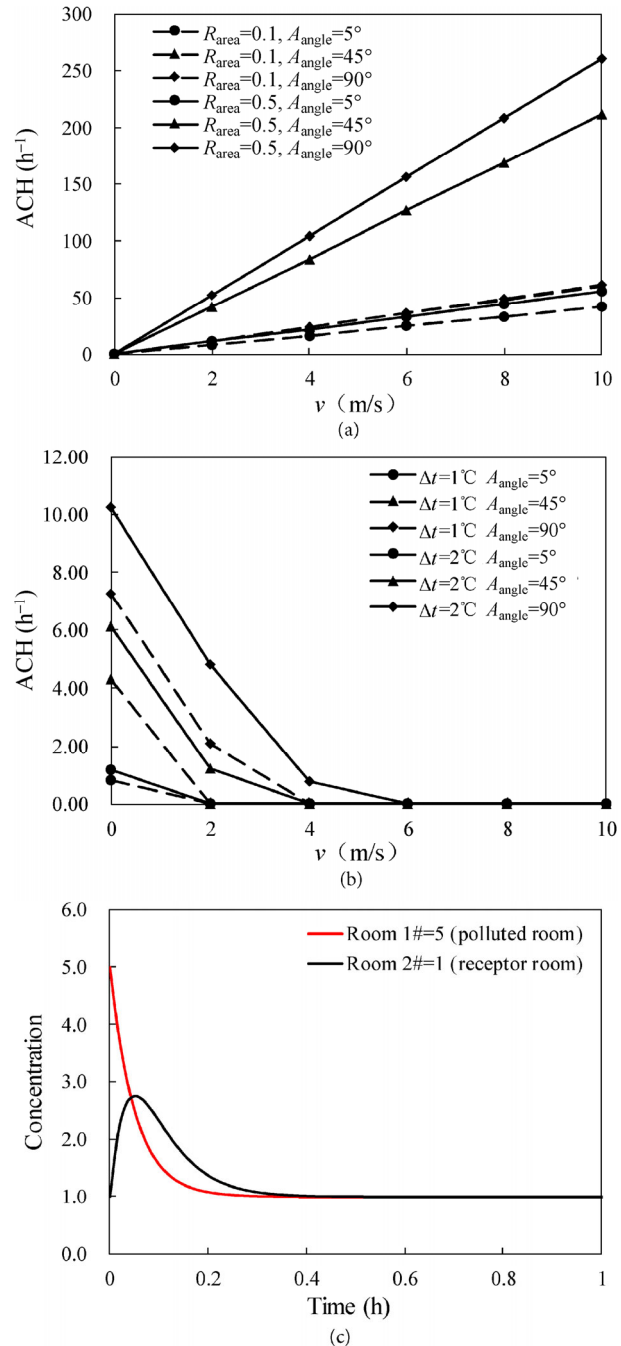


Fig. 5 ACH and indoor pollutant simulation results of the two-room model using the exterior window open and interior door open behavior. (a) ACHs from outdoor to Room 1#, Room 1# to Room 2#, and Room 2# to outdoor with $\Delta t = 0\text{ }^\circ\text{C}$; (b) ACH from Room 2# to Room 1# with $R_{\text{area}} = 0.1$; (c) indoor pollutant variations of the rooms with $\Delta t = 0\text{ }^\circ\text{C}$ at $A_{\text{angle}} = 5^\circ$

When there was a temperature difference, the airflow and ventilation rate from outdoor to Room 1# were almost the same as those without a temperature difference (Fig. 5(a)). Two-way airflows only occurred at the interior door and exterior window of Room 2# under low wind velocities ($v < 6$ m/s). The ACHs from Room 2# to Room 1# at $R_{\text{area}} = 0.1$ are illustrated in Fig. 5(b). The larger the opening angle and temperature difference are, the larger the two-way airflow rate is. The ACH from Room 2# to Room 1# decreased rapidly with the increases in outdoor wind velocity and opening area ratio of the exterior window. The two-way airflow only occurred at $v = 0$ m/s when the opening area ratio of the exterior window (R_{area}) increased to 0.5. By comparing the ACH from Room 2# to Room 1# with the ACH from outdoor to Room 1# (Fig. 5(b) vs. Fig. 5(a)), one can conclude that the ventilation rate of the room was mainly dominated by the air exchange with the outdoors in most cases, especially for situations with high outdoor wind velocity.

When $\Delta t = 0$ °C, only the scenario with a polluted Room 1# was simulated. Pollutant concentrations at $R_{\text{area}} = 0.1$, $A_{\text{angle}} = 5^\circ$, and $v = 4$ m/s are shown in Fig. 5(c). The ACH was 16.7 h^{-1} for this case. The indoor pollutant concentration of Room 1# decreased very quickly, within several minutes, to the same level it was outdoors. The pollutant was transported from Room 1# to Room 2# increased in concentration in the first few minutes, and then decreased. The concentration differences between rooms were obvious initially, but the concentrations decreased to the same level as outdoors in tens of minutes, after which the difference was negligible. When there is a temperature difference, the two-way airflow rate was much lower than the mainstream airflow in most cases, thus indoor pollutant variations were similar.

From a pollutant removal perspective, double-sided ventilation was more effective than single-sided ventilation. Due to the large ACH and rapid decline characteristics of the pollutant concentration under the exterior windows and interior door open scenario, the opening area or angle of the window/door need not be kept large, and the ventilation time could be reduced to several to tens of minutes from indoor pollutant removal and energy saving perspectives.

3.1.4 Exterior window closed and interior door closed

The ACHs from outdoor to Room 1#, Room 1# to Room 2#, and Room 2# to outdoor with $\Delta t = 0$ °C are shown in Fig. 6(a). The ACH for this situation was the smallest among all the window/door opening behaviors. Both the air tightness of the interior door and exterior window affected the ventilation rate.

When there were temperature differences, two-way airflow only occurred at the interior door under low wind velocity when C_{ew} was small and C_{ed} was large (e.g., $C_{\text{ew}} = 0.3 \text{ cm}^2/\text{m}^2$, $C_{\text{ed}} = 12 \text{ cm}^2/\text{m}^2$), or at the exterior window of Room 2# when

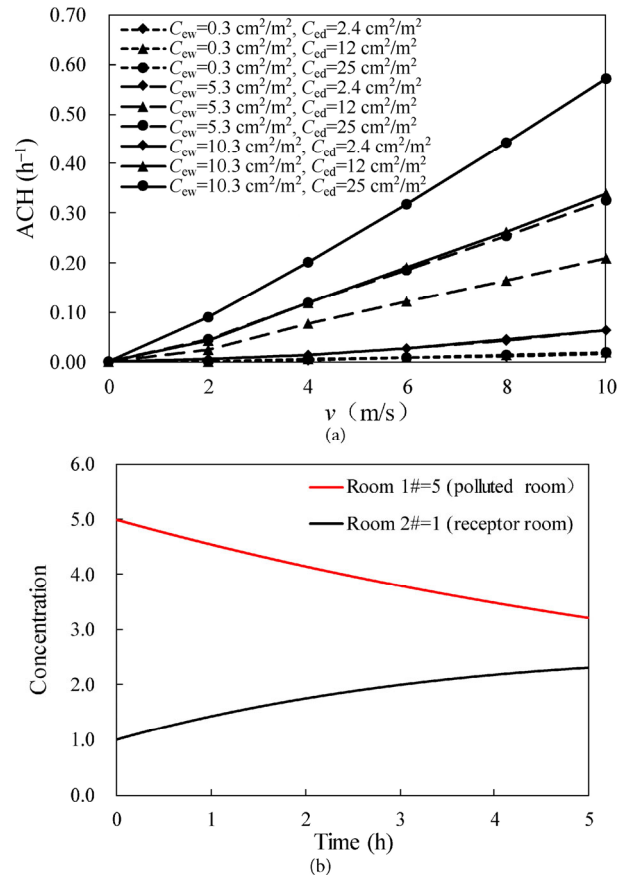


Fig. 6 ACH and indoor pollutant simulation results of the two-room model using the exterior window closed and interior door closed behavior. (a) ACHs from outdoor to Room 1#, Room 1# to Room 2#, and Room 2# to outdoor with $\Delta t = 0$ °C; (b) indoor pollutant variations of the rooms with $\Delta t = 0$ °C

C_{ew} was large and C_{ed} was small (e.g., $C_{\text{ew}} = 10.3 \text{ cm}^2/\text{m}^2$, $C_{\text{ed}} = 2.4 \text{ cm}^2/\text{m}^2$). The two-way airflow rates were smaller than $1 \text{ m}^3/\text{h}$, which was in the same magnitude as that reported by Miller and Nazaroff (2001). The ACHs from outdoor to Room 1#, Room 1# to Room 2#, and Room 2# to outdoor were almost the same as those when no temperature difference was present.

As mentioned above, the airflow and ACH of the rooms were the same in most cases between the occasions with or without temperature differences under this window/door opening behavior. Thus, only the pollutant concentrations without temperature differences were analyzed. Indoor pollutant variations at $C_{\text{ew}} = 5.3 \text{ cm}^2/\text{m}^2$, $C_{\text{ed}} = 25 \text{ cm}^2/\text{m}^2$, and $v = 4$ m/s with ACH = 0.12 h^{-1} were simulated and are illustrated in Fig. 6(b). The indoor pollutant concentration of Room 1# decreased and that of Room 2# increased. The change tendencies were the slowest and the concentration differences were the largest among all the window/door opening behaviors. The two-room residence could not be treated as a well-mixed zone. The pollutant could not be eliminated effectively.

3.2 Experimental and simulation results of the three-room residence

3.2.1 Boundary conditions and airflow results

To simulate indoor CO₂ variation and validate the airflow characteristics for different experimental scenarios, the airflow of the three-room experimental residence was first simulated by CONTAM. Outdoor wind direction and speed, and outdoor and indoor temperatures are the required boundary conditions. During the experiment, outdoor wind and temperature varied from time to time. Indoor temperature was relatively stable when the windows and doors were closed but varied when the windows were opened. Given that the measurement durations were relatively short (~1 h), the prevailing outdoor wind direction and corresponding wind speed and average indoor and outdoor temperatures were used in the CONTAM airflow analysis. This simplification may cause some discrepancies between the simulation and measurement results, but the general variation trend could be presented well. In the first experimental scenario, the prevailing outdoor wind direction was from the east and the corresponding average wind speed was 0.48 m/s. The average outdoor temperature was 4.5 °C and the average temperatures in Rooms 1#, 2# and 3# were 9.9 °C, 12.8 °C, and 11.1 °C, respectively. Wind direction and speed in the second experimental scenario were different from the first one. The prevailing wind was from the north and the average wind speed was 8 m/s. The average outdoor temperature was 0 °C and the average indoor temperatures in Rooms 1 #, 2#, and 3# were 2.9 °C, 8.1 °C, and 9.8 °C, respectively. The airflow models in Section 2.2 were used in this three-room residence analysis.

Airflow simulation results for the first experimental scenario showed that the main stream of air was from outdoor to Room 1#, Room 2# to Room 3# and Room 3# to outdoor. Strong two-way airflow occurred at the interior door of Room 1# (D_{int}1) due to the temperature difference and the large opening angle. The airflow rates from Room 1# to Room 2# and Room 2# to Room 1# were 321 m³/h and 256 m³/h, respectively. The airflow rates from Room 2# and Room 3# to outdoor were 50 m³/h and 17 m³/h, respectively, much larger than those vice versa (< 1 m³/h), suggesting that the two-way airflow barely occurred at the closed openings. The airflow rates in the second experimental scenario were higher than those in the first one because of the opened windows and reduced flow resistance. The airflow rates from outdoor to Room 1#, Room 1# to Room 2# and Room 2# to Room 3# were 890 m³/h, 933 m³/h, and 40 m³/h, respectively. The airflow rate from Room 2# to Room 1# was 41 m³/h, much less than the flow rate in the

reverse direction (933 m³/h). The two-way airflow was inhibited during the exterior window and interior door open scenario, even the temperature difference between Room 1# and Room 2# was 5.2 °C. Two-way airflow occurred at the opened exterior window of Room 3#. The airflow rates from Room 3# to outdoor and outdoor to Room 3# were 65 m³/h and 25 m³/h, respectively.

3.2.2 Indoor CO₂ measurement and simulation results

The indoor CO₂ concentrations of the experimental scenarios were simulated and are presented in Fig. 7 with the measurement results. In the first experimental scenario (Fig. 7(a)), concentration differences between Room 1-1# and Room 1-2# are not significant, suggesting that the well-mixed assumption was reasonable within a room. When D_{int} 1 was opened, the indoor CO₂ concentration in Room 1# increased and that in Room 2# decreased. CO₂ was

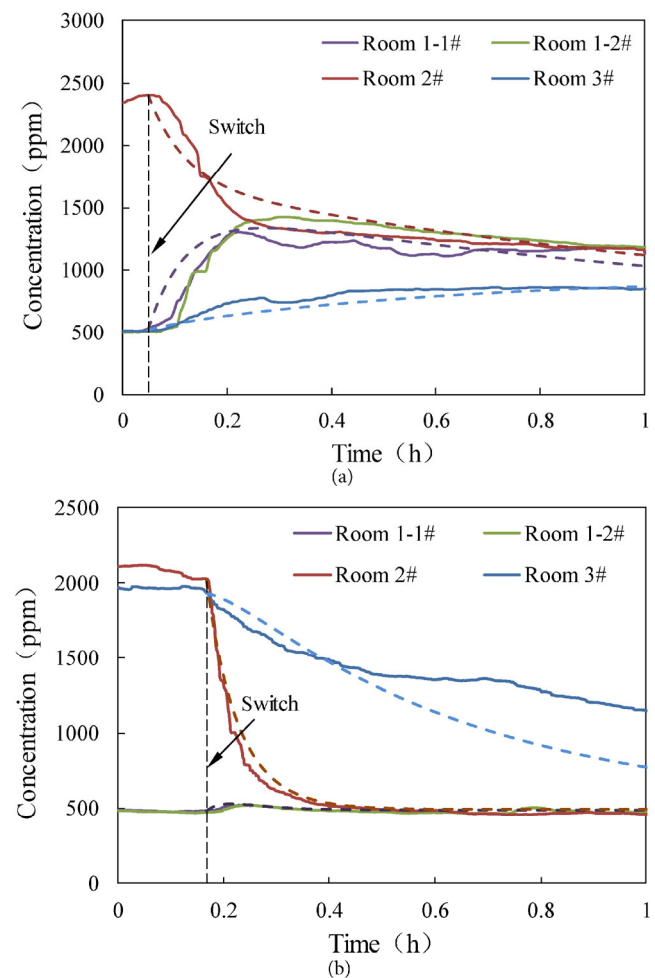


Fig. 7 Indoor CO₂ measurement and simulation results of the rooms under different window/door opening behaviors. (a) The first experimental scenario; (b) the second experimental scenario (the solid and dash lines are the measurement and simulation results, respectively)

transported from Room 2# to Room 1# and the air was well mixed within 0.2 h, according to the measurement data. The variation patterns were similar to the simulation results presented in Fig. 4(c) as well. The simulation results of CO₂ in Room 2# decreased faster at the beginning of the measurement and then more slowly than the measurement data. This discrepancy may have been induced by the simplification of the variable outdoor wind and temperature conditions for the airflow analysis. Concentration variations in Rooms 2# and 3# could be used to analyze the pollutant transport under the exterior window closed and interior door closed behavior, which shared the same patterns as the simulation results in Fig. 6(b). The simulation results for Room 3# agreed well with the measurement data. These good agreements between the measurement and simulation results indicate the accuracy of the simulation results.

According to the measurement data of the second experimental scenario (Fig. 7(b)), when $W_{\text{ext } 1}$, $D_{\text{int } 1}$ and $W_{\text{ext } 2}$ were opened, Rooms 1# and 2# are under the exterior window open and interior door open behavior. Compared to the first experimental scenario, indoor CO₂ concentration in Room 2# decreased much faster, indicating a larger ACH. Moreover, the CO₂ concentration in Room 1# remained at almost the same level before and after switching the window/door positions, and only a limited amount of CO₂ was transported from Room 2# to Room 1#. The simulation results for Room 1# and Room 2# agreed well with the measurement data. The concentration in Room 3# decreased more slowly than that in Room 2#, indicating a smaller ventilation rate in the room. Thus, the conclusion that the room with single-sided ventilation has a lower ventilation rate than the double-sided ventilation was verified. Moreover, after opening the window for tens of minutes ($t > 0.4$ h), the CO₂ concentration in Room 2# decreased to the same level as outdoors, whereas the CO₂ concentration in Room 3# was still high, but was not transported to Room 2#. Field experimental results for Rooms 2# and 3# also confirm that opening the exterior window of the polluted room and closing the interior door could effectively remove the pollutant and prevent its transport between rooms. The simulation results for Room 3# decreased faster than the measurements did, which indicates the airflow rate of Room 3# was overestimated. However, the overall variation trend and pollutant transport by the airflow were well represented by the simulation results.

4 Conclusions

In this study, exterior and interior airflows and indoor pollutant variations under different window/door opening behaviors were analyzed. Field experiments were also

performed and the main conclusions were validated by measurement data. The conclusions drawn are as follows.

- (1) The ventilation rate of the room was the largest when the exterior windows and interior door were open and the smallest when the exterior window and interior door were closed. The ACH was smaller than 1 h^{-1} and increasing the opening area/angle of the window/door had little effect when the room had single-sided ventilation and lack of a temperature difference.
- (2) If there was no temperature difference, the airflows through all the openings were unidirectional under different window/door opening behaviors. If there was a temperature difference, two-way airflows could barely occur when all the windows and doors of the residence were closed or open. There was a concentration difference between rooms and the two-room residence could not be simplified to a well-mixed zone.
- (3) A temperature difference could induce two-way airflows at the exterior window (interior door) when the exterior window was open (closed) and the interior door was closed (open). The two-way airflow rate increased about 40% when the temperature difference increased from $1 \text{ }^\circ\text{C}$ to $2 \text{ }^\circ\text{C}$. The strong two-way airflow drove pollutant transport between rooms and the air in the two connected rooms was well mixed after the interior door was opened for tens of minutes.
- (4) From an indoor pollutant control perspective, increasing the number of openings is more effective than increasing the opening area when the room has single-sided ventilation. Opening the exterior window of the polluted room and closing the interior door could remove pollutants and prevent pollutant transport to clean rooms simultaneously when a temperature difference is present.

Acknowledgements

The research was supported financially by the national key project of the Ministry of Science and Technology, China on "Green Buildings and Building Industrialization" through Grant No. 2016YFC0700500.

References

- ASHRAE (2001). ASHRAE Handbook—Fundamentals, Chapter 26. Atlanta, GA: American Society of Heating, Refrigerating and Air-Conditioning Engineers.
- Brasche S, Bischof W (2005). Daily time spent indoors in German homes—Baseline data for the assessment of indoor exposure of German occupants. *International Journal of Hygiene and Environmental Health*, 208: 247–53.
- Baughman AV, Gadgil AJ, Nazaroff WW (1994). Mixing of a point source pollutant by natural convection flow within a room. *Indoor Air*, 4: 114–122.

- Canha N, Mandin C, Ramalho O, Wyart G, Ribéron J, Dassonville C, Hänninen O, Almeida SM, Derbez M (2016). Assessment of ventilation and indoor air pollutants in nursery and elementary schools in France. *Indoor Air*, 26: 350–365.
- Chen C, Zhao B, Yang X, Li Y (2011). Role of two-way airflow owing to temperature difference in severe acute respiratory syndrome transmission: Revisiting the largest nosocomial severe acute respiratory syndrome outbreak in Hong Kong. *Journal of the Royal Society Interface*, 8: 699–710.
- Chen C, Zhao B, Weschler CJ (2012a). Indoor exposure to “outdoor PM10”: Assessing its influence on the relationship between PM10 and short-term mortality in U.S. cities. *Epidemiology*, 23: 870–878.
- Chen C, Zhao B, Zhou W, Jiang X, Tan Z (2012b). A methodology for predicting particle penetration factor through cracks of windows and doors for actual engineering application. *Building and Environment*, 47: 339–348.
- Du L, Batterman S, Godwin C, Rowe Z, Chin JY (2015). Air exchange rates and migration of VOCs in basements and residences. *Indoor Air*, 25: 598–609.
- Dols WS, Emmerich SJ, Polidoro BJ (2016). Coupling the multizone airflow and contaminant transport software CONTAM with EnergyPlus using co-simulation. *Building Simulation*, 9: 1–11.
- Dodson RE, Levy JI, Shine JP, Spengler JD, Bennett DH (2007). Multi-zonal air flow rates in residences in Boston. *Atmospheric Environment*, 41: 3722–3727.
- Dols WS, Walton GN, Denton KR (2013). CONTAMW 2.0 User Manual—Multizone Airflow and Contaminant Transport Analysis Software. Gaithersburg, MD, USA: National Institute of Standards and Technology.
- Emmerich SJ, Howard-Reed C, Naginger SJ (2004). Validation of multizone IAQ model predictions for tracer gas in a townhouse. *Building Services Engineering Research and Technology*, 25: 305–316.
- Ferro AR, Klepeis NE, Ott WR, Nazaroff WW, Hildemann LM, Switzer P (2009). Effect of interior door position on room-to-room differences in residential pollutant concentrations after short-term releases. *Atmospheric Environment*, 43: 706–714.
- Howard-Reed C, Wallace LA, Ott WR (2002). The effect of opening windows on air change rates in two homes. *Journal of the Air and Waste Management Association*, 52: 147–59.
- Isaacs K, Burke J, Smith L, Williams R (2013). Identifying housing and meteorological conditions influencing residential air exchange rates in the DEARS and RIOPA studies: development of distributions for human exposure modeling. *Journal of Exposure Science and Environmental Epidemiology*, 23: 248–258.
- Johnson T, Myers J, Kelly T, Wisbith A, Ollison W (2004). A pilot study using scripted ventilation conditions to identify key factors affecting indoor pollutant concentration and air exchange rate in a residence. *Journal of Exposure Analysis and Environmental Epidemiology*, 14: 1–22.
- Liang W, Yang X (2013). Indoor formaldehyde in real buildings: Emission source identification, overall emission rate estimation, concentration increase and decay patterns. *Building and Environment*, 69: 114–120.
- McGrath JA, Byrne MA, Ashmore MR, Terry AC, Dimitroulopoulou C (2014). A simulation study of the changes in PM_{2.5} concentrations due to interzonal airflow variations caused by internal door opening patterns. *Atmospheric Environment*, 87: 183–188.
- Miller SL, Nazaroff WW (2001). Environmental tobacco smoke particles in multizone indoor environments. *Atmospheric Environment*, 35: 2053–2067.
- Nantka MB (2005). Airtightness and natural ventilation: A case study for dwellings in Poland. *International Journal of Ventilation*, 4: 79–91.
- Nabi S, Flynn MR (2015). Buoyancy-driven exchange flow between two adjacent building zones connected with top and bottom vents. *Building and Environment*, 92: 278–291.
- Ott WR, Klepeis NE, Switzer P (2003). Analytical solutions to compartmental indoor air quality models with application to environmental tobacco smoke concentrations measured in a house. *Journal of the Air and Waste Management Association*, 53: 918–936.
- Persily A, Musser A, Emmerich SJ (2010). Modeled infiltration rate distributions for U.S. housing. *Indoor Air*, 20: 473–485.
- Shi S, Chen C, Zhao B (2015). Air infiltration rate distributions of residences in Beijing. *Building and Environment*, 92: 528–537.
- Teclé A, Bitsuamlak GT, Jiru TE (2013). Wind-driven natural ventilation in a low-rise building: A Boundary Layer Wind Tunnel study. *Building and Environment*, 59: 275–289.
- Tlili O, Mhiri H, Bournot P (2015). Effect of chimney design on flow induced by a heat source in a room. *Building Simulation*, 8: 567–577.
- Taheri M, Schuss M, Fail A, Mahdavi A (2016). A performance assessment of an office space with displacement, personal, and natural ventilation systems. *Building Simulation*, 9: 89–100.
- Viegas JC, Nogueira S, Aelenei D, Cruz H, Cano M, Neuparth N (2015). Numerical evaluation of ventilation performance in children day care centres. *Building Simulation*, 8: 189–209.
- Wilson AL, Colome SD, Tian Y, Becker EW, Baker PE, Behrens DW, Billick IH, Garrison CA (1996). California residential air exchange rates and residence volumes. *Journal of Exposure Analysis and Environmental Epidemiology*, 6: 311–326.
- Weber DD, Kearney RJ (1980). Natural convective heat transfer through an aperture in passive solar heated buildings. In: Proceedings of 5th National Passive Solar Conference, Amherst, MA, USA, pp. 1037–1041.
- Yang C, Shi H, Yang X, Zhao B (2010). Research on flow resistance characteristics with different window/door opening angles. *HVAC & R Research*, 16: 813–824.